transferred by forced siphon using argon pressure through a cannula into an argon-flushed centrifuge tube capped with a septum stopper. The suspension of the catalyst was centrifuged and the supernatant was removed by forced siphon under argon using a cannula. The precipitate containing the catalyst was washed twice with 25-mL portions of toluene and the washings were checked by GC for cyclooligomerization products. After two washings no products were detected. Dry toluene (30 mL) was added to the precipitated catalyst, and then the resulting slurry of catalyst was transferred back to the Lab Crest pressure bottle described above. The cyclooligomerization reaction was repeated using only a fresh charge of butadiene and heating the suspension to 95 °C for 5 h. The separation, recovery, and recycling of the catalyst was continued three times.

Determination of Nickel Leached from the Catalyst. Nickel in the product solution from the second cycle of a cyclooligomerization carried out in the presence of the oligomeric phosphite ligand **6a** was determined in the following way: A weighed sample of about 1–2 g of the supernatant from the second cycle of this cyclooligomerization was evaporated in a 20-mL porcelain crucible. Concentrated H_2SO_4 (1 mL) was added to the residue and the crucible was gently heated on a hot plate for 2 h until the residue was completely decomposed. When 70% HNO_3 (1 mL) was added dropwise followed by further heating on the hot plate for 15–20 h with occasional shaking of the contents. A clear pale yellow solution was obtained after the acid digestion was diluted with distilled water to 25 mL in a volumetric flask. The resulting solution was analyzed by ICP[24] and showed that the leachate contained 5 ppb of Ni, which corresponds to <0.01% of the nickel in the initial catalyst charge.

Acknowledgment is made to the donors of the Petroleum Research Fund, administered by the American Chemical Society, the Robert A. Welch Foundation, and the Texas A&M Center for Energy and Mineral Resources for funding of this research.

Registry No. **7a**, 100781-90-6; **7b**, 105281-83-2; **7c**, 100781-89-3; **11b**, 105281-84-3; **11c**, 105281-85-4; COD, 111-78-4; VCH, 100-40-3; CDT, 676-22-2; 4-MeO$C_6H_4CH_2Cl$, 824-94-2; 4-MeOC_6H_4MgCl, 699-19-4; I$(CH_2)_9CH_3$, 629-93-6; 4-MeO$C_6H_4(CH_2)_{18}CH_3$, 105281-80-9; 4-HO$C_6H_4(CH_2)_{18}CH_3$, 105281-81-0; 2-PhC_6H_4OH, 90-43-7; (2-Ph$C_6H_4O)_2$PCl, 105281-82-1; ClP$(OEt)_2$, 589-57-1; ClP$(OPh)_2$, 5382-00-3; (2-$CH_2)_{17}CH_3$, 26762-44-7; triphenyl phosphite, 101-02-0; tris(*o*-tolyl) phosphite, 2622-08-4; tris(*o*-biphenylyl) phosphite, 2752-19-4; ethylene, 74-85-1; butadiene, 106-99-0.

---

[24] Shanina, T. M.; Gel'man, N. E.; Mikhailovskaya, V. S.; Kabaeva, N. M. *Zh. Anal. Khim.* **1981**, *36*, 414–417.

Disproportionation of Quinone Radical Anions in Protic Solvents at High pH[1]

David O. Wipf, Kenneth R. Wehmeyer, and R. Mark Wightman*

Department of Chemistry, Indiana University, Bloomington, Indiana 47405

Received April 10, 1986

The voltammetry of anthraquinone, anthraquinone-2-sulfonate, and anthraquinone-2,6-disulfonate has been examined in aqueous and alcoholic solutions with tetraethylammonium hydroxide as the supporting electrolyte. At basic values of pH, the product of the two-electron reduction of each of these species is the dianion. The reduction process is found to proceed in two well-defined, one-electron steps in basic 2-propanol and ethanol. In basic methanol the two one-electron waves virtually overlap, and complete wave overlap is observed in basic aqueous solution. The differences in the half-wave potentials for the one-electron steps have been used to calculate the equilibrium constant for disproportionation of the radical anions in each solution. The logarithm of the equilibrium constant is found to correlate directly with the ability of the solvent to hydrogen bond, as determined by regression against Taft's scale of hydrogen-bond donor acidities. Thus, these data clearly show the strong influence of solvent–anion interactions on the thermodynamics of the reduction steps for anthraquinones.

Electron-transfer reactions that involve quinones, hydroquinones, and catechols are important in many areas of chemistry, especially in biological systems. Thus, it is not surprising that the thermodynamic parameters that govern these reactions have been studied extensively by pulse radiolysis[2] and electrochemical techniques.[3] Electron spin resonance has been used to demonstrate the presence of quinone radicals as intermediates in the redox processes of hydroquinones in aqueous solution.[4,5] The radical intermediates have been characterized with UV-visible spectroscopy following pulse radiolysis in aqueous solutions.[2,6-9] These measurements have been used to determine the acidity constants of radicals[10] and to provide an indirect measure of the standard reduction potentials ($E°$) for the one-electron processes.

Scheme I

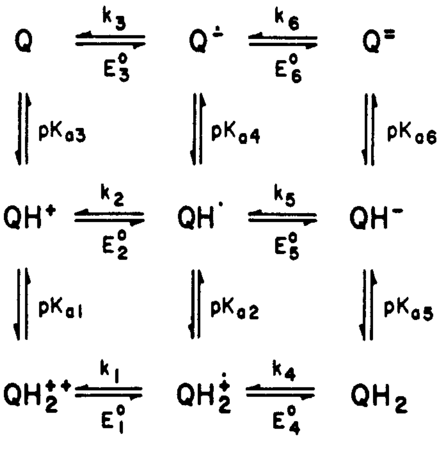

The nine-member box scheme (Scheme I) summarizes the possible intermediates for all two-electron, two-proton

---

[1] This research was supported by the National Science Foundation (CHE-85-00529).

[2] Ilan, Y. A.; Czapski, G.; Meisel, D. *Biochim. Biophys. Acta* **1976**, *430*, 209.

[3] Chambers, J. A. *Chemistry of the Quinoids, Part 2*; Patai, S., Ed.; Wiley: New York, 1974; Chapter 14.

[4] Meisel, D.; Czapski, G. *J. Phys. Chem.* **1975**, *79*, 1503.

[5] Meisel, D.; Fessenden, R. W. *J. Am. Chem. Soc.* **1976**, *98*, 7505.

[6] Meisel, D.; Neta, P. *J. Am. Chem. Soc.* **1975**, *97*, 5198.

[7] Willson, R. L. *Trans. Faraday Soc.* **1971**, *67*, 3020.

[8] Steenken, S.; Neta, P. *J. Phys. Chem.* **1979**, *83*, 1134.

[9] Steenken S.; Neta, P. *J. Phys. Chem.* **1982**, *86*, 3661.

[10] Willson, R. L. *J. Chem. Soc. D* **1971**, 1249.

0022-3263/86/1951-4760$01.50/0 © 1986 American Chemical Society

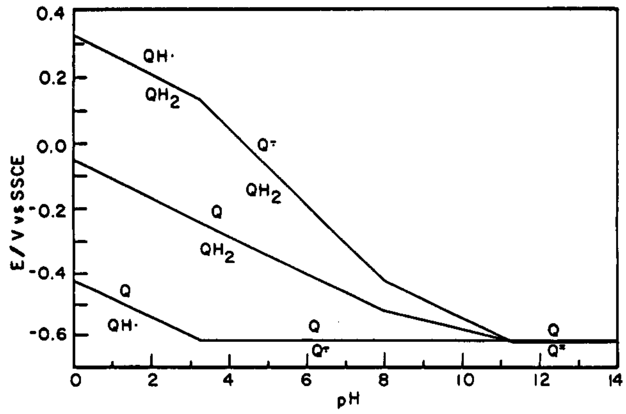

Figure 1. Pourbaix diagram for AQS in water. Center line corresponds to the net two-electron reduction. The lower line is the one-electron reduction process to form the radical anion. The upper line is the one-electron reduction process to form the dianion. The pK_a values for the hydroquinone (11.3 and 8.0) and the $E°$ values for the two-electron reduction are from ref 16. The one-electron $E°$ values and the semiquinone pK_a (3.2) are from ref 6.

reactions such as the quinone/hydroquinone couple. Given the relevant thermodynamic parameters, the mostly likely intermediates can be identified at a particular pH and represented in a Pourbaix diagram (Figure 1). The actual mechanism of reaction depends on the relative rates of proton and electron transfer.[11] Scheme I has been used successfully to interpret the voltammetry of several quinone systems at intermediate pH.[12-15]

The nine-member box scheme (Scheme I) indicates that at very high pH values in protic solvents, protonations are unimportant, and that the observed electron-transfer reactions should be affected only by electron-transfer kinetics and the $E°$s of the relevant couples. Under these conditions the redox chemistry in basic, protic solvents should resemble that found in aprotic solvents, where the radical anion is known to be thermodynamically stable for a wide number of disparate quinones.[3] The data in Figure 1 suggest that this is not the case, since the $E°$s for the formation of the radical anion and dianion are similar, and thus the equilibrium constant for disproportionation of the radical anion must be close to unity. To identify the participation of the role of the solvent in the disproportionation process, we have examined the first and second reduction processes of a series of anthraquinones in several protic solvents, at high values of pH. The equilibrium constants for the disproportionation of the relevant radical anion have been determined from the voltammetric data. Mercury ultramicroelectrodes have been employed so that the reduction processes can be examined over a wide range of time scales.

Experimental Section

Electrodes. Platinum microdisk electrodes were prepared by sealing 2.0-μm radius wire (Goodfellow Metals, U.K.) into soft glass. These electrodes were coated with a mercury hemisphere (5.5-μm radius) by electrodeposition as described previously.[17] The platinum electrodes were polished with 0.05-μm alumina (Beuhler, Lake Bluff, IL) before use in each experiment. The reference electrode employed throughout was a saturated sodium calomel electrode (SSCE).

Apparatus. The electrochemical cell was a 25-mL screw-top vial with holes drilled in the cap for electrode placement and gas purging. The potentiostat employed for fast-scan cyclic voltammetry was of a two-electrode configuration and was designed and constructed locally. Simple, two-electrode potentiostats can be used with ultramicroelectrodes because of the small effects of *iR* drop.[18-20] The potentiostat has a minimum time constant of 0.3 μs at the lowest gain setting. To maximize the high frequency response, special consideration was given to stray capacitance of the instrument. Switches were not employed in the current-to-voltage transducer, and the lead to the working electrode was kept short (4 cm). The current transducer stage was mounted on a separate circuit board adjacent to the electrochemical cell. The gain was adjusted by replacing the value of the feedback resistor. LFP357 operational amplifiers (National Semiconductor) were used in the current-to-voltage conversion stage and in a subsequent amplification stage. All experiments were conducted inside a Faraday cage grounded to earth.

Waveforms for cyclic voltammetry were generated by a Wavetek Model 143 function generator (San Diego, CA). Data were collected with a digital oscilloscope (Nicolet 320, Madison, WI). The oscilloscope can be used to store scans from solutions without an electroactive species for subsequent subtraction. It also has the facility for performing a five-point, moving average smooth of the data. After collection the data was sent to a digital plotter (model 7074A, Hewlett-Packard) for permanent record.

Procedure. Solutions were deoxygenated for at least 15 min with high-purity argon or nitrogen before use. The suporting electrolyte used in protic solvents was tetraethylammonium hydroxide (TEAOH). Cations such as K^+ can cause a positive shift in the reduction potential for the dianion in nonaqueous[21] solutions due to ion-pairing phenomena. Background scans were recorded immediately after recording a scan in the depolarizer solution and were subtracted to remove contibutions from residual current.[22]

The $E°'$s were obtained from the half-wave potentials obtained at slow scan rates when well-separated waves were observed. When distinct waves were observed only at fast scan rates, the $E°'$s were estimated as the midpoint of the forward and reverse waves. To examine the number of electrons transferred at each wave (*n*), voltammograms were recorded under conditions of spherical and linear diffusion. These two conditions allow separation of *n* from the diffusion coefficient.

Digital simulations of cyclic voltammetry with planar diffusion were performed on an IBM PC (IBM, Boca Roton, FL) using a standard-finite-difference method. A three-point approximation was used to simulate the flux at the electrode surface. Planar diffusion models are suitable for ultramicroelectrodes of the size used here for sweep rates greater than 200 V s^{-1}.[18] Nonlinear regression employed a simplex procedure,[23] and correlation coefficients were evaluated as described in ref 24.

Reagents. Methanol (HPLC grade, Fisher, Fairlawn, NJ), ethanol (Absolute, AAPER Alcohol and Chemical Co., Shelbyville, KY), and 2-propanol (Mallinckrodt, Paris, KY) were used as received. Water was distilled, ion-exchanged, and distilled a second time with a Corning Mega-Pure water purification system (Corning, NY). Tetraethylammonium hydroxide (10% w/v in water or 25% w/v in methanol; Kodak, Rochester, NY) was employed throughout as the supporting electrolyte. The quinones tested are all stable in this media for several hours.[25] Anthraquinone-2-sulfonate (AQS) (ICN Pharmaceuticals, Plainview, NY)

---

(11) Laviron E. *J. Electroanal. Chem.* **1984**, *169*, 23.

(12) Laviron, E.; Roullier, L. *J. Electroanal. Chem.* **1983**, *157*, 7.

(13) Laviron, E. *J. Electroanal. Chem.* **1984**, *164*, 213.

(14) Deakin, M. R.; Wightman, R. M. *J. Electroanal. Chem.* **1986**, *206*, 167.

(15) Deakin, M. R.; Stutts, K.; Kovach, P. M.; Wightman, R. M. *Anal. Chem.* **1986**, *58*, 1474.

(16) Clark, W. M. *Oxidation-Reduction Potentials of Organic Systems*; Williams and Wilkins: Baltimore, MD, 1974.

(17) Wehmeyer, K. R.; Wightman, R. M. *J. Electroanal. Chem.* **1985**, *57*, 1989.

(18) Howell, J. O.; Wightman, R. M. *Anal. Chem.* **1984**, *56*, 524.

(19) Bond, A. M.; Fleischmann, M.; Robinson, J. *J. Electroanal. Chem.* **1984**, *168*, 299.

(20) Howell, J. O.; Wightman, R. M. *J. Phys. Chem.* **1984**, *88*, 3915.

(21) Peover, M. E. *Electroanalytical Chemistry*; Bard, A. J., Ed. Marcel Decker: New York, 1973; Vol. 2.

(22) Bond, A. M. *Modern Polarographic Methods in Analytical Chemistry*; Marcel Decker: New York, 1980.

(23) Aberg, E. R.; Gustavsson, A. G. T. *Anal. Chim. Acta* **1982**, *144*, 39.

(24) Wilford, J. H.; Archer, M. D. *J. Electroanal. Chem.* **1985**, *190*, 271.

(25) Bailey, S. I.; Ritchie, I. M. *Electrochim. Acta* **1985**, *30*, 3.

Table I. Voltammetric Properties of Anthraquinones in Different Solvents

	AQ			AQS			2,6-AQS		
	slope, mV[c]			slope, mV[c]			slope, mV[c]		
solvent	1st wave	2nd wave	$\Delta E_{1/2}$, mV	1st wave	2nd wave	$\Delta E_{1/2}$, mV	1st wave	2nd wave	$\Delta E_{1/2}$, mV
2-propanol	60	58	−205 ± 6	57	62	−256 ± 9	67	56	−279 ± 2
ethanol	59	57	−164 ± 10	67	54	−164 ± 10	65	55	−179 ± 18
methanol	71	*a*		67	*a*	−82 ± 4	107	*a*	−88 ± 1
water				70	*a*	−9[b]	68	*a*	

[a] Only one wave observed. [b] Reference 6. [c] Slopes by linear regression of the data according to eq 2.

and anthraquinone-2,6-disulfonate (2,6-AQS) (Aldrich) were recrystalized from water. Anthraquinone (AQ) (Kodak) was recrystallized from ethanol.

Results

Voltammetry in Basic 2-Propanol. Voltammograms for AQS and AQ at slow-scan rates at a mercury ultramicroelectrode exhibit two consecutive waves. The voltammograms have a sigmoidal shape because of the predominance of spherical diffusion to the electrode. The limiting current (i_d) for each wave under these conditions is given by[17]

$$i_d = 2\pi rnFDC \tag{1}$$

where r is the electrode radius in cm, n is the number of electrons, F is the Faraday constant, D is the diffusion coefficient, and C is the concentration in mol/cm^3. Equation 1 provides a simple method to determine the product of the diffusion coefficient and the number of electrons. In addition, the shape of an electrochemically reversible voltammetric wave under these conditions is given by[26]

$$E = E_{1/2} + 2.303RT/nF \log ((i_d - i)/i) \tag{2}$$

where i is the current on the rising part of the voltammetric wave, and $E_{1/2}$ is the half-wave potential. Thus, a plot of E vs. the current function for each wave should give a straight line with a slope of 59 mV for a reversible one-electron wave at room temperature. This is found to be the case for both waves of each of the quinones in basic 2-propanol (Table I). The diffusion coefficients for AQ and AQS in this media calculated with the use of eq 1 for the first, one-electron wave are $D = 7 \times 10^{-6}$ and 2×10^{-6} cm^2 s^{-1}, respectively. The separation in $E_{1/2}$ values also is given in Table I.

The voltammograms of AQ and AQS in basic 2-propanol at scan rates above 200 V s^{-1} are characterized by two well-defined reduction waves. At rapid sweep rates the voltammetry is dominated by linear diffusion.[27] A reverse wave is associated with each reduction wave, which indicates a chemically reversible process. In addition, the half-wave potential, estimated from the separation of the forward and reverse wave, is within 2–5 mV of that obtained with slower scans where spherical diffusion predominates. The amplitude of the waves increases linearly with the square root of scan rate (v), indicative of a diffusion-controlled process. Digital simulations of the first voltammetric wave can be used to evaluate the number of electrons transferred under conditions of linear diffusion. With the use of the n value from eq 2 and the diffusion coefficient calculated from eq 1, a good fit is obtained. The data at rapid scan rates provide an alternate method to determine the two parameters of interest, n and D. The peak current under conditions of linear diffusion is proportional to $n^{3/2}D^{1/2}$[25] while the limiting current is proportional to nD. This property of ultramicroelectrodes has been used for similar purposes with chronoamperometric data.[28]

The solubility of 2,6-AQS in basic 2-propanol is limited, so fast-scan voltammograms were precluded. However, the separation of the first and second reduction waves could be obtained from the slow-scan-rate voltammograms. These waves have the wave shape expected for a one-electron process (Table I).

Voltammetry in Basic Ethanol. Voltammograms of AQ, AQS, and 2,6-AQS in basic ethanol at slow scan rates at a mercury ultramicroelectrode exhibit two consecutive waves. Analysis of the the wave shapes by eq 2 gives the expected slopes for a reversible, one-electron wave for each of the waves (Table I). Calculation of the diffusion coefficient with eq 1 gives $D = 9 \times 10^{-6}$, 4×10^{-6}, 3×10^{-6} cm^2 s^{-1} for AQ, AQS, and 2,6-AQS, respectively.

At scan rates greater than 200 V s^{-1} two reversible reduction waves are observed. However, the separation of the two waves in ethanol is reduced with respect to the separation seen in 2-propanol (Table I). Simulation of the current response using the n and D value from the slow-scan data also indicate the waves are each one electron.

Voltammetry in Basic Methanol. Voltammograms of AQ, AQS, and 2,6-AQS at slow-scan rates give a single wave for each of these compounds (Figure 2). If the waves are assumed to be two electron, the calculated diffusion coefficients are 1×10^{-5}, 7×10^{-6}, 6×10^{-6} cm^2 s^{-1}, respectively. Analysis of the wave shapes using eq 2 indicates slopes larger than predicted for either a one- or a two-electron process (Table I). This would occur with two consecutive reduction processes whose waves are separated by less than 90 mV.

Voltammograms at scan rates of 200 V s^{-1} provide greater evidence for the presence of two, separate waves for AQS and 2,6-AQS (Figure 2). Discrimination of adjacent waves is more likely at fast scan rates since the wave position is determined by interfacial electron-transfer kinetics as well as the $E^{\circ\prime}$'s. For the voltammetry of AQS, the simulations agree with two overlapping one-electron waves. The fit for 2,6-AQS is not so good, but shows a similar trend. In contrast, a good fit to a simulation involving two, one-electron waves or one, two-electron wave is not obtained for AQ, suggesting an intermediate case. One-electron voltammetric waves separated by 36 mV or greater add as the sum of the two processes[29] and thus the separation of the waves for AQ must be less than this value in basic MeOH. The separation of the $E_{1/2}$ values for AQS and 2,6-AQS were determined from these data, and are given in Table I.

Voltammetry in Basic Aqueous Solution. Voltammograms for AQS and 2,6-AQS in basic aqueous solution at slow scan rates at a mercury ultramicroelectrode have

---

(26) Bard, A. J.; Faulkner, L. *Electrochemical Methods; Fundamentals and Applications*; Wiley: New York, 1980.

(27) Nicholson, R. S.; Shain, I. *Anal. Chem.* **1964**, *36*, 706.

(28) Baranski, A. S.; Fawcett, W. R.; Gilbert, C. M. *Anal. Chem.* **1985**, *57*, 166.

(29) Ammar, F.; Saveant, J. M. *J. Electroanal. Chem.* **1973**, *47*, 215.

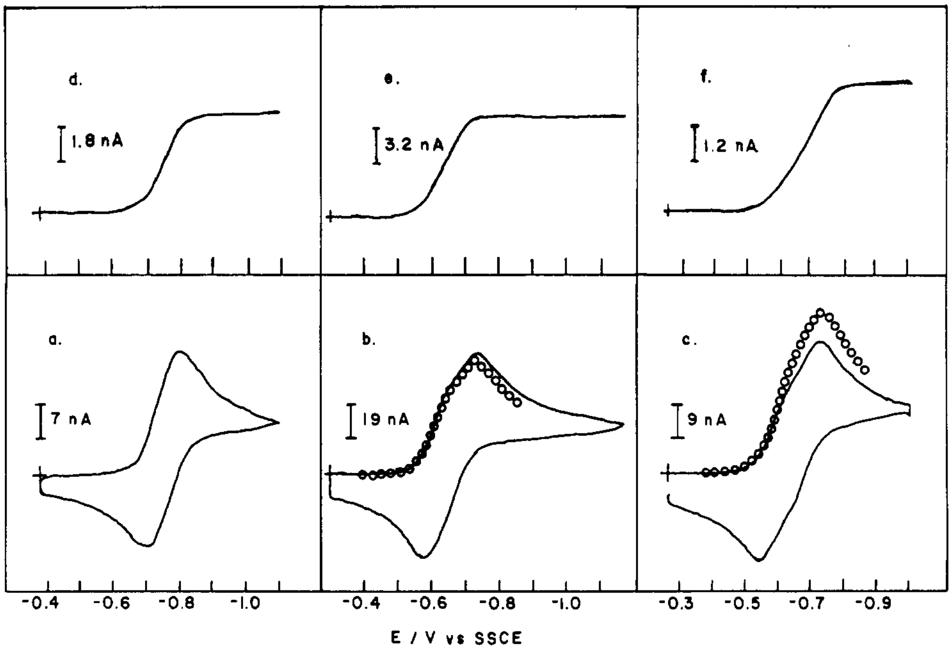

Figure 2. Cyclic voltammograms in methanol at a 5.5-μm radius mercury ultramicroelectrode with 0.1 M TEAOH supporting electrolyte. (a) 0.5 mM AQ, $v = 200$ V s^{-1}. (b) 2.0 mM AQS, $v = 200$ V s^{-1}. Open circle indicates the sum of the current response of two superimposed digital simulations. $\alpha = 0.5$, $k° = 0.4$ cm s^{-1}, $D = 7 \times 10^{-6}$ cm^2 s^{-1}. (c) 1.0 mM 2,6-AQS, $v = 200$ V s^{-1}. (d) Open circles as in (b) for $\alpha = 0.5$, $k° = 0.2$ cm s^{-1} (e) 2.0 mM AQS, $v = 10$ mV s^{-1}. (f) 1.0 mM 2,6-AQS, $v = 10$ mV s^{-1}.

a single, sigmoidal wave (assuming $n = 2$, then $D = 5 \times 10^{-6}$ and 4×10^{-6} respectively). Analysis of the wave shapes by eq 2 gives straight-line curves. The measured slope could reflect two closely associated one-electron waves consistent with the Pourbaix diagram constructed for AQS (Figure 1).

The voltammograms of AQS at scan rates above 200 V s^{-1} are characterized by single, well defined reduction waves whose amplitude increases linearly with the square root of scan rate (v) as expected for a diffusion-controlled process. A second wave occurs at more negative potentials, but this wave exhibits the characteristics expected for the reduction of a species adsorbed at the electrode surface (i.e., nonlinear dependence on $v^{1/2}$). Digital simulation of the diffusion-controlled voltammetric wave using the diffusion coefficient from the steady-state response indicates that the peak current is twice the height expected for a one-electron process, rather than a single two-electron process. Thus, the data indicate that the voltammetric response for AQS is a convolution of two, closely spaced one-electron waves. This conclusion is identical with results from pulse radiolysis experiments which show a difference in the reduction potential for the quinone and the radical anion of 9 mV at basic pH.[6]

Cyclic voltammetry at fast-scan rates in aqueous solution is limited to AQS due to the insolubility of AQ and the severe adsorption of 2,6-AQS at a mercury electrode.

Discussion

From the voltammetric data it is clear that the separation of the $E_{1/2}$ values for the two, one-electron reductions of this series of anthraquinones decreases in the order 2-propanol > ethanol > methanol > water. For reversible electron transfers with couples which have equal diffusion coefficients, $E_{1/2}$ is identical with the $E°$ for the half reaction. The measured values are therefore related to the equilibrium constant (K_{disp}) for disproportionation of the radical anion, $2Q^{\cdot-} \rightleftharpoons Q + Q^{2-}$, by

$$\ln K_{\mathrm{disp}} = (nF/RT)(E_2° - E_1°) \qquad (3)$$

where $E_1°$ and $E_2°$ are the one-electron standard reduction potentials for the quinone and radical anion respectively. Thus, the measured values are a direct measure of the stability of the radical anion in each solution with respect to disproportionation. Furthermore, since the supporting electrolyte was constant in all of these experiments, and since the pH value was sufficiently high that the dianion is the two-electron product of these reductions, the solvent is the primary cause of the observed changes in equilibria.

Correlation of the half-wave potentials for the first, one-electron reduction of several quinones with various different solvent polarity scales have been reported.[24,30] These correlations rely on finding a suitable reference couple to transfer data from half-cell reactions between solvents. However, the direct measurement of free energies for disproportionation allows correlation with solvent effects on disproportionation without this type of assumption. Therefore, we have examined a number of solvent parameters to determine a correlation with the observed behavior. In addition to the measured values, we have used reported values for the peak separation of AQ and AQS in dimethylformamide and acetonitrile in tetraethylammonium-ion solutions.[3,20,31]

The best correlation has been found with the numerical scale developed by Taft and co-workers referred to as the α_{1-14} scale of solvent hydrogen-bond donor acidities.[32,33] This scale provides a measure of the hydrogen-bond donation and excludes the polarity contribution from solvent to substrate molecules. An excellent correlation is obtained between this scale and the logarithm of K_{disp} for AQS ($r = 0.999$, $n = 6$, Figure 3). In this plot equilibrium constants are included which are calculated from data obtained in aqueous solutions from pulse radiolysis observations. The data in Table I for AQ and 2,6-AQS show good correlations with the α_{1-14} scale as well ($r = 0.991$, $n = 4$, and 0.997, $n = 3$, respectively). The chemical sig-

---

(30) Jaworski, J. S.; Lesniewska, E.; Kalinkowski, M. K. *J. Electroanal. Chem.* **1979**, *105*, 329.

(31) Chen, K. S.; Hirota, N. *J. Am. Chem. Soc.* **1972**, *94*, 5550.

(32) Taft, R. W.; Kamlet, M. J. *J. Am. Chem. Soc.* **1976**, *98*, 2886.

(33) Taft, R. W.; Kamlet, M. J. *J. Chem. Soc., Perkin Trans. 2* **1979**, 1723.

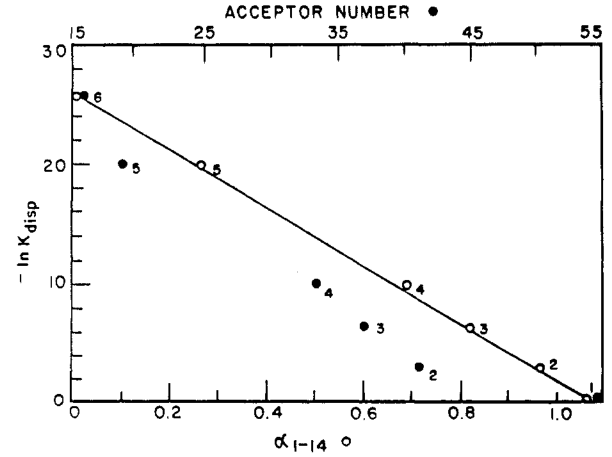

Figure 3. Plot of the negative logarithm of K_{disp} for the reduction of AQS in various solvents vs. the acceptor number (closed circles[34,35]) and α_{I-14} (open circles[32,33]) scales of solvent polarity. Numbers indicate the solvent: 1, water; 2, methanol; 3, ethanol; 4, 2-propanol; 5, acetonitrile; and 6, dimethylformamide.

nificance of this correlation is substantiated by reports from other laboratories. Hydrogen-bonded radical anions of anthraquinone with 2-propanol have been directly observed by electron spin resonance.[31] Furthermore, hydrogen-bonded intermediates have been implicated in kinetic studies of anthraquinone radical anion protonation.[34]

Two other solvent parameters have been correlated with the data in Table I. The Gutman acceptor number[35,36] is a measure of the Lewis acidity of the solvent, and so should reflect the ability to solvate anions. Linear regression of the data for AQS with this parameter gave a poorer correlation ($r = 0.963$) with the data point from aqueous solutions giving the largest deviation. Swain's A and B numbers,[37] which have been obtained by extensive correlation with many solvent processes, are associated with anion and cation solvating ability, respectively. The data in Table I were fit to Swain's numbers using nonlinear regression with the following expression:

$$\ln K_{disp} = aA + bB + c \qquad (4)$$

The ratio of b/a for the best fit was −0.29 with a correlation coefficient of 0.992. It is interesting to note that Swain finds that the α term of Taft is best expressed by a similar ratio, −0.36. This further suggests that hydrogen-bonding acidity is a major reason for the observed changes in disproportionation equilibria.

The high degree of correlation of the thermodynamic data with hydrogen-bonding donicity and the poor correlation of a solvent scale that relates to solvent polarity (i.e., the Gutman number) indicates that hydrogen bonding is the major factor in the observed changes in stability of the radical anion in protic solvents at very high values of pH. Solvents which form stronger hydrogen bonds facilitate disproportionation. The high sensitivity of the equilibrium constant to solvent effects in part reflects the greater stabilization of the dianion by hydrogen bonding. In addition, the radical anion is destabilized with respect to disproportionation by charge delocalization from hydrogen bonding. For benzoquinone it has been shown that the former is the greater effect.[24] The correlation for hydrogen bonding is sufficiently high that predictions of stability in other, untested solvents may be readily applicable. Thus, for the first time, it should be possible to extrapolate the large amount of electrochemical data obtained in aprotic solvents to aqueous solutions. Furthermore, hydrogen bonding may be important in the observed disproportionation of other radicals. For example, oxygen shows similar electrochemical behavior in basic, aqueous solution, and the superoxide anion can be stabilized by an organic layer at the electrode surface.[38]

Registry No. AQ, 84-65-1; AQS, 84-48-0; 2,6-AQS, 84-50-4.

---

(34) Wightman, R. M.; Cockrell, J. R.; Murray, R. W.; Burnett, J. N.; Jones, S. B. *J. Am. Chem. Soc.* **1976**, *98*, 2562.

(35) Mayer, U.; Gutmann, V.; Gerger, W. *Monatsh. Chem.* **1975**, *106*, 1235.

(36) Gutmann, V. *Coord. Chem. Rev.* **1976**, *18*, 225.

(37) Swain, C. G.; Swain, M. S.; Powell, A. L.; Alunni, S. *J. Am. Chem. Soc.* **1983**, *105*, 502.

(38) Chevalet, J.; Roulle, R.; Gierst, L.; Lambert, J. P. *J. Electroanal. Chem.* **1972**, *39*, 201.

Kinetics and Mechanism of the Oxidation of Substituted Benzaldehydes by *N*-Bromobenzamide

Kalyan K. Banerji

Department of Chemistry, University of Jodhpur, Jodhpur 342 001, India

Received March 11, 1986

The oxidation of eighteen meta- and para-substituted benzaldehydes by *N*-bromobenzamide (NBB), to the corresponding benzoic acid, is first order with respect to the aldehyde, NBB, and hydrogen ion. The oxidation of benzaldehyde exhibited a substantial primary kinetic isotope effect ($k_H/k_D = 5.3 \pm 0.1$). Addition of benzamide has no effect on the reaction rate. $(PhCONH_2Br)^+$ has been postulated as the reactive oxidizing species. The rates of the oxidation of meta- and para-substituted benzaldehydes were separately correlated in Taft's and Swain's dual substituent parameter equations. For para-substituted aldehydes, the best correlation was obtained with σ_I and σ_R^+ values, while meta-substituted compounds correlate with σ_I and σ_R^0 values. The reaction constants have negative values. A mechanism involving transfer of a hydride ion from the aldehyde to the oxidant, in the rate-determining step, has been proposed.

Kinetics of the oxidation of organic compounds by *N*-halogeno amides have received considerable attention recently.[1-8] Similarly the oxidations of aromatic aldehydes by transition-metal ions have been reported.[9] There seems

0022-3263/86/1951-4764$01.50/0 © 1986 American Chemical Society